Proceedings of the IEEE-EMBS International Conference on Biomedical and Health Informatics (BHI 2012)
Hong Kong and Shenzhen, China, 2-7 Jan 2012

A Novel EMD-Based Common Spatial Pattern for Motor Imagery Brain-Computer Interface

Wei He, Pengfei Wei, Liping Wang and Yuexian Zou

***Abstract*—Common Spatial Pattern (CSP) algorithm is a commonly used effective feature extraction method in motor imagery (MI) electroencephalogram (EEG) based brain computer interface (BCI). The motor imagery patterns extracted by CSP are associated with variations in subject-specific frequency bands power. Therefore, optimizing frequency band carrying MI intention is required by the CSP method. However, the frequency band is usually divided manually and evaluated which does make use of the EEG signal property and also with low efficiency. In this paper, we propose a novel Empirical Mode Decomposition (EMD) based CSP method to realize the data-related and adaptive frequency band selection. Specifically, the intrinsic mode functions (IMFs) decomposed from the EMD and the amplitude modulated signal by instantaneous amplitude (IA) calculated from Hilbert Transform have been fully explored and employed. Moreover, the intensive experiments have been conducted to evaluate the proposed method. From the experiment results, we observed that the EMD based CSP method enhances the classification accuracy in BCI competition IV dataset I for all subjects and a paired t-test shows a significant difference level.**

I. Introduction

Brian Computer Interface (BCI) are systems that provide an alternative pathway for their users to transmit information to external world, which has become an assistive tool for neuromuscular disordered people's communication and control [1]. Electroencephalogram (EEG) signal recoded from the scalp could well reflect the brain activities and it has been widely used in noninvasive BCI systems [2]. One kind of effective EEG-based BCI system uses the potential changes in motor imagery (MI) termed as MI-based BCI. And these changes detected by EEG signal during imagination of a movement manifest as a rhythmic power decrease and increase in primary sensor-motor areas which is known as event-related desynchronization (ERD) and event-related synchronization (ERS) [3].

A particularly popular signal processing algorithm for MI-based BCIs called Common Spatial Pattern (CSP) [4] is employed to detect the ERD/ERS characterized motor imagery intention. The traditional CSP method used in the binary-class constructs spatial filters that maximize the variance of one kind of task and simultaneously minimize the variance of another which could be accomplished by solving a generalized eigenvalue decomposition problem [5]. In order to achieve high classification accuracy (CA), a pre-filtered broad band (8-30Hz) or subject-specific frequency bands (μ and β bands) most reflecting the MI intention are selected. To find these optimal frequency bands, several algorithms have been proposed, such as CSSP (Common Spatio-Spectral Pattern) [6], Sub-band CSP (SBCSP) [7] and Filter Bank Common Spatial (FBCSP) [8]. These methods aim at determining the informative frequency bands and the features are extracted accordingly which can also be weighted to achieve high classification accuracy.

In this paper, we propose a novel method employing the Empirical Mode Decomposition (EMD) [9] to automatically and effectively detect the discriminative and informative frequency bands signal. EMD method was pioneered by N.E. Huang et al. in 1998 and only uses the original signal for decomposition. Hence it is a fully data-driven and self-adaptive analysis approach [10]. It adaptively represents non-stationary signals as a sum of zero mean amplitude modulation frequency modulation components termed as the intrinsic mode functions (IMFs). The EMD method could behave as filter banks and different IMFs is able to reflect the inherent information in the original EEG signal [11]. It is desired to note that the first two IMFs (termed as IMF1, IMF2) are mainly related to the optimal informative frequency bands (alpha band and beta band) which contain the MI intention.

Hence, the use of the filter property of EMD could avoid manually dividing the frequency band, which is usually adopted in the traditional CSP method. Moreover, it can be expected that a few number of informative frequency band related IMFs will lead to higher algorithm efficiency. The proposed method has been tested and evaluated by using the BCI competition IV dataset I calibration data, where five subjects out of seven are used who preformed left hand and right hand imagination tasks. The dataset for each subject comprises 200 trials (100 for each class) and the EEG signal is sampled at 1000Hz from 59 electrodes.

Manuscript received November 10, 2011. The work was funded by the National Basic Research Program of China (973program:2009CB526501, 2010CB529605), Guangdong Innovation Research Team Fund for Low-cost Healthcare Technologies, Science and Technology Funds of Guangdong Province (2009B030801037)

W. He. is with Shenzhen Key Lab of Neuropsychiatric Modulation, Shenzhen Institutes of Advanced Technology, Chinese Academy of Sciences, Shenzhen 518055, China and Advanced Digital Signal Processing Laboratory Peking University Shenzhen Graduate School Shenzhen 518055, China weo.he@siat.ac.cn

P. Wei. is with Shenzhen Key Lab of Neuropsychiatric Modulation, Shenzhen Institutes of Advanced Technology, Chinese Academy of Sciences, Shenzhen 518055, China pf.wei@siat.ac.cn

L. Wang is with Shenzhen Key Lab of Neuropsychiatric Modulation, Shenzhen Institutes of Advanced Technology, Chinese Academy of Sciences, Shenzhen 518055, China lp.wang@siat.ac.cn

Y. Zou is with Advanced Digital Signal Processing Laboratory Peking University Shenzhen Graduate School Shenzhen 518055, China zouyx@szpku.edu.cn

II. PROPOSED METHOD

Thirty-seven electrodes over the primary motor cortex and the supplementary motor cortex (SMA) were selected from the total fifty-nine electrodes and the block diagram of the proposed method was illustrated in Fig. 1. The detailed description of each block will be addressed separately in the following context.

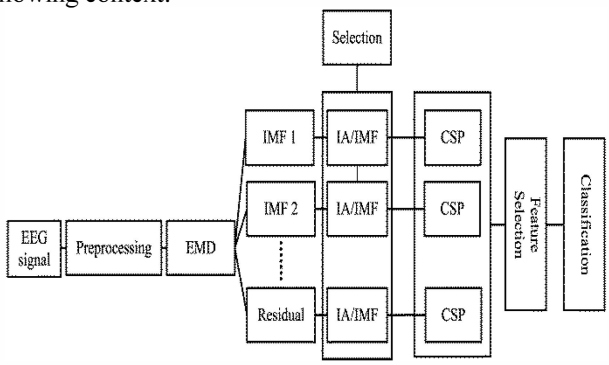

Fig. 1 Block diagram of the proposed method

A. Preprocessing

The raw EEG signal was re-referenced by a common average referencing (CAR) spatial filter and was filtered with a 5-order Butterworth band pass filter with the pass band of 5-40 Hz.

B. Common Spatial Pattern Algorithm

The CSP algorithm analyzes multi-channel EEG data and yields spatial filters $W_{csp} \in R^{C\times C}$ (C is the number of channels) which project the original signal to a space where the differences in variances of two kinds of tasks can be maximized. The projected signal is given by:

$$Z_{csp}(t) = WE(t) \tag{1}$$

where $E(t) \in R^{C\times T}$ represents the raw EEG signal of a single trial (T indicates the length of the samples). Then the CSP features could be calculated as [5]:

$$f_p = \log\left(\frac{\mathrm{var}(Z_p)}{\sum_{i=1}^{2m}\mathrm{var}(Z_i)}\right) \quad p = (1\cdots 2m) \tag{2}$$

where Z_p indicates the first m and last m rows of Z_{csp} . The value of m was set to be 3 in this paper.

C. Empirical Mode Decomposition

In principle, the EMD method decomposes the given signal $X(t)$ into residual and intrinsic modes which ends up in the form of [12]:

$$X(t) = \sum_{i=1}^{N} c_i(t) + r_n(t) \tag{3}$$

where $r_n(t)$ indicates a residual and $c_i(t), i = 1,...N$ stands for the IMFs. The zero-mean amplitude IMFs are obtained by a sifting process according to the characterizing conditions of the IMFs and the process can be finished when residual becomes a monotonic component or a constant where no more IMFs component can be extracted. The IMFs have well-behaved Hilbert transforms, so the instantaneous frequencies and instantaneous amplitude could be calculated as follows [9]:

$$\tilde{c}_i(t) = \frac{1}{\pi} p.v \int_{-\infty}^{+\infty} \frac{c_i(\tau)}{t-\tau} d\tau \tag{4}$$

$$a_i(t) = \sqrt{c_i^2(t) + \tilde{c}_i^2(t)} \tag{5}$$

$$\theta_i(t) = \arctan\frac{\tilde{c}_i(t)}{c_i(t)} \tag{6}$$

$$\omega_i = \frac{d\theta_i(t)}{dt} \tag{7}$$

where $\tilde{c}_i$ is the Hilbert transform of c_i and $p.v$ denotes the Cauchy principal value. Then, the instantaneous frequencies and instantaneous amplitude are determined as ω_i and $a_i(t)$ respectively.

D. IA modulated Signal/IMFs selection approach

We explore to evaluate the nature of the extracted IMFs and IA. An approach to form the input signal to the CSP using IA information is explored. The instantaneous amplitude (IA) information of the IMFs can be used to modulate a sinusoidal signal as:

$$x_{IA}(t) = a(t)\cos(2\pi f_c(t)) \tag{8}$$

where $a(t)$ indicates IA and f_c is the frequency of the modulated signal. An example of the IMF with IA and the amplitude modulated signal was shown in Fig. 5, where f_c was select at 500Hz and the function $\cos(2\pi f_c(t))$ would be of the oscillation property so the inner product of the signal x_{IA} and $a(t)$ is the same:

$$X_{IA}(t)X_{IA}^T(t) = a(t)a^T(t) \tag{9}$$

Moreover, in this study, the first three IMFs and the combination of them are selected to be the input to the CSP since they hold the informative frequency bands related to the ERD/ERS. To evaluate the impact of the selection of IMFs or IA on the CA, several experiments have been conducted in the next section.

E. Feature Selection

In the feature selection stages, the fisher ratio is taken as the measure to discriminate the features, which is defined as follows:

$$S_B = \sum_{i=1}^{C} N_i(M_i - M)^2 \tag{10}$$

$$S_W = \sum_{i=1}^{C}\sum_{t=1}^{N_i}(f_t - M_i)^2 \tag{11}$$

$$F = \frac{S_B}{S_W} \tag{12}$$

where M_i is the mean value of the features for class i , N_i is the number of trials for class i, f_t is the feature for one trial

in one class. M is the mean value of the total classes. The higher value of the Fisher ratio defined in (12) indicates the higher discriminative property of this set of the features.

In this study, the fisher ratios of the features computed by the CSP method for individual use of the IMFs or IA have been calculated, respectively. The most discriminative features can be selected corresponding to the largest fisher ratios. All the feature dimensions are selected to be equal among the method for fair comparison.

F. Classification

A linear support vector machine (SVM) classifier is adopted as the classifier. The final CA is the mean value of the result from a 5×5-fold cross-validation procedure. The data lasting two seconds was selected (2.5s to 4.5s after the cue) to calculated the CSP features.

III. Result and Discussion

In this section, in order to evaluate and compare the performance of the EMD based the CSP methods, 13 different methods have been tested. The results of the CA are shown in Table I. In Table 1, the CSP, CSP-alpha and CSP-beta represent the filtered signal between 8-30Hz, 8-13Hz 18-26Hz as the input to CSP, respectively. The IMF1, IMF2, IA1, and IA2 refer to the individual IMF1, IMF2, the amplitude modulated signal by IA1 and IA2 as the input to CSP, respectively. The IMF1+IMF2, IMF1+IMF2+IMF3, IA1+IA2 and IA1+IA2+IA3 denote the combination of the IMF1+IMF2, IMF1+IMF2+IMF3, IA1+IA2 and IA1+IA2+IA3 as the input to the CSP, respectively. The IMF fisher ratio and the IA fisher ratio indicate that the input of CSP is selected by the fisher ratio defined in (12), respectively.

TABLE I
CLASSIFICATION ACCURACIES CORRESPONDING TO THE PROPOSED METHOD AND NORMAL CSP METHOD (%)

Subject	A	B	C	D	E	Mean
CSP	60.0±2.7	64.8±2.8	86.9±1.4	92.3±2.1	92.1±1.0	79.22
CSP-alpha	59.0±3.6	67.9±2.9	77.8±4.2	88.8±1.0	91.2±1.3	76.94
CSP-beta	54.8±1.8	50.3±2.2	70.0/2.2	75.8±1.1	92.1±1.6	68.60
IMF1	54.3±1.6	55.0±2.4	74.7±1.8	87.3±1.6	83.0±1.3	70.86
IMF2	58.6±4.1	66.4±1.3	61.4±4.3	88.9±0.9	85.4±1.4	72.14
IMF1+IMF2	67.7±2.2	70.0±1.2	83.9±1.3	93.0±1.2	93.2±1.2	81.56
IMF1+IMF2+IMF3	66.5±1.6	68.3±1.9	88.7±1.5	93.8±1.7	93.4±0.8	82.14
IMF fisher ratio	55.4±2.8	65.4±3.3	72.8±2.6	93.5±2.3	88.4±1.6	75.10
IA1	50.8±2.3	54.0±2.5	70.1±1.9	78.7±1.8	86.1±1.9	67.94
IA2	59.1±4.1	67.3±2.4	61.2±3.6	82.9±2.9	81.6±1.4	70.42
IA1+IA2	57.6±3.0	59.4±0.5	66.3±3.0	87.3±1.9	94.2±1.2	72.96
IA1+IA2+IA3	65.1±2.4	70.2±3.2	70.7±4.1	92.2±1.3	94.8±0.6	78.60
IA fisher ratio	59.7±3.3	61.5±1.4	71.2±3.2	90.2±1.2	90.4±1.6	74.60

From the experimental results show in Table I, we can see that the CA of the IMF1+IMF2 and the IMF1+IMF2+IMF3 is higher than the CSP. Moreover, a paired t-test was computed resulting in a significant difference level between the IMF1+IMF2+IMF3 and CSP ($P = 0.0403$). However, the IMF1+IMF2 failed to reflect a significant different level compared with the CSP. We can infer that the IMF3 should contain the MI intention information contributing to the classification. To further illustrate the classification performance of the IMFs based methods, the CA results of the IMF1, IMF2, IMF1+IMF2, IMF1+IMF2+IMF3 are plotted in Fig. 3, respectively. From Fig. 3, it is clear to see that the CA of the IMF1+IMF2 is higher than that of IMF1 and IMF2 for each subject. We also noted that the CA of the IMF1+IMF2+ IMF3 is higher for subject C, D, and E, but is lower for subject A and B compared with that of the IMF1+IMF2. These would suggest that the IMF1 and IMF2 extracted by EMD method indeed contain the information of MI intention for each subject. Meanwhile, whether the IMF3 component reflects the MI intention is subject-dependent determined by the subject-based predominant ERD/ERS frequency bands. The ERD phenomenon of the IMF3 for subject C in C3 and C4 channels were shown in Fig. 4. From Fig. 4, it is clear to see there is a power decrease in the low alpha band during left hand task but the ERD phenomenon is a relative unobvious during right hand task.

From Table I, it is also noted that the CA of the IMF1 and IMF2 is still lower than the CSP-alpha and the CSP-beta for majority of the subjects. This further justifies that the frequency components in the IMFs are overlapped and not restrict to the frequency band [8]. Therefore, it is nature to conclude that a single IMF is not able to reflect the MI intention sufficiently. This also contributes to the lower CA of the IMF fisher ratio method.

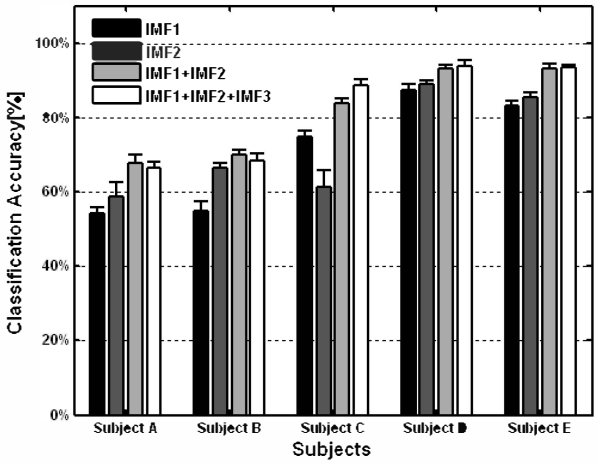

Fig. 3 Bar graph comparing the classification performance of the method of different combination of IMFs

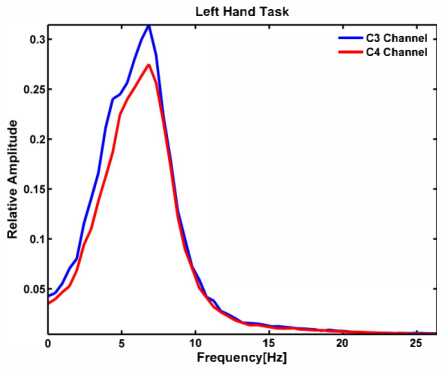

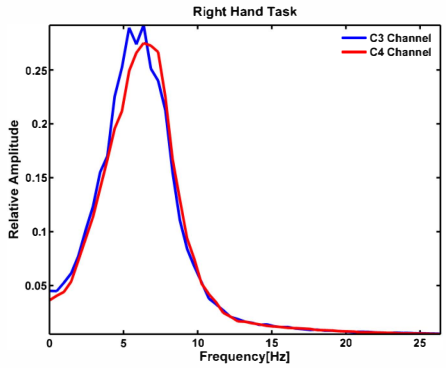

Fig. 4 Average spectrum of the IMF3 of subject C for C3 and C4 channel during left hand task and right hand task.

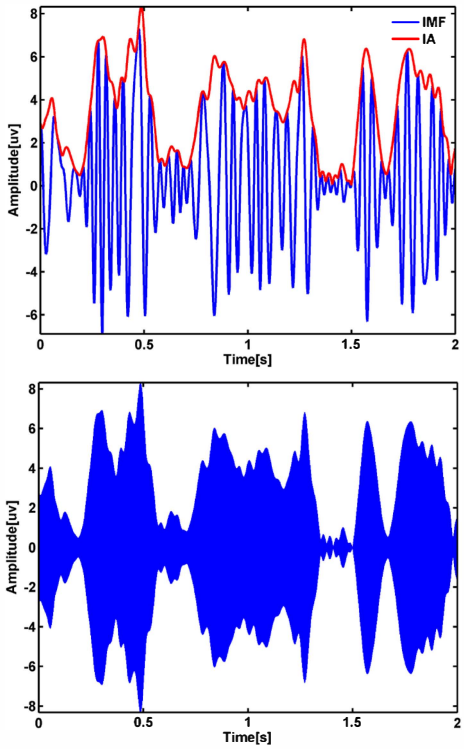

Fig .5 IMF with IA (top) and amplitude modulated signal (bottom) for one trial of subject E

From Table I, we can see that the CA of IA1+IA2+IA3 is higher for four subjects (A, B, D and E). None of the IA based method enhances the CA of the subject C. Carefully analysis and experimental results show that the CA of the IA based CSP method may be impacted by the selection of the modulation frequency. The IA modulated signal may not a good representation of the MI intention for all subjects. Moreover, as the IMFs method, the individual IA fails to completely convey the IM intention for all subjects as well. Therefore, how to make use of the IA for representation of the MI intention is needed to be further investigated.

IV. Conclusion

In this paper, we employed the EMD method to extract the IMFs and IAs of the EEG signal and a novel EMD-based CSP method for the classification of the MI EEG signals has been proposed. The fusion of the EMD and CSP utilized the filter bank property of EMD which is able to adaptively extract the IMFs of the signal that carrying MI intention to satisfy the optimizing frequency band selection requirement in the CSP method. Experimental results show that the IMFs-based CSP method results in higher CA using BCI competition IV dataset I. However, the IA-based CSP method fails to increase the CA since the information contained in the amplitude modulated signal is insufficient. One of the advantages of the proposed EMD based CSP method lies in its self-adaptive IMFs extraction where the number of IMFs is data-related and limited. This property greatly increases the algorithm efficiency.

Furthermore, the frequency components contained in different IMFs are different in the identical location but the adjacent IMFs could contain the same scale oscillations. It means that the decomposition is not strict to the frequency band but according to inherent physical meaningful components in the original signal. Therefore, extracting and combining MI intention contained components in raw EEG signal not merely according to the different frequency division but to find the inherent informative signal components might be efficiency and meaningful.

V. Acknowledgment

The author would like to thank the Berlin BCI group: Berlin Institute of Technology and Fraunhofer FIRST, and Campus Benjamin Franklin of the Charité - University Medicine Berlin, Department of Neurology, Neurophysics Group for providing the data sets used in BCI Competition IV.

Reference

[1] G. P. a. G.R. Müller-Putz, et al., "Rehabilitation with Brain-Computer Interface Systems," IEEE Computer Society 2008.
[2] J. R. Wolpaw, et al., "Brain-computer interfaces for communication and control," Clinical Neurophysiology, vol. 113, pp. 767-791, Jun 2002.
[3] G. Pfurtscheller and F. H. L. d. Silvab, "Event-related EEG/MEG synchronization and desynchronization: basic principles," Clinical Neurophysiology, 1999.
[4] H. Ramoser, et al., "Optimal spatial filtering of single trial EEG during imagined hand movement," Rehabilitation Engineering, IEEE Transactions on, vol. 8, pp. 441-446, 2000.
[5] B. Blankertz, et al., "Optimizing spatial filters for robust EEG single-trial analysis," Signal Processing Magazine, IEEE, vol. 25, pp. 41-56, 2008.
[6] G. Dornhege, et al., "Combined Optimization of Spatial and Temporal Filters for Improving Brain-Computer Interfacing," Biomedical Engineering, IEEE Transactions on, vol. 53, pp. 2274-2281, 2006.
[7] Q. Novi, et al., "Sub-band common spatial pattern (SBCSP) for brain-computer interface," pp. 204-207.
[8] K. K. Ang, et al., "Filter bank common spatial pattern (FBCSP) in brain-computer interface," 2008, pp. 2390-2397.
[9] N. E. Huang, et al., "The empirical mode decomposition and the Hilbert spectrum for nonlinear and non-stationary time series analysis," Proceedings of the Royal Society of London. Series A: Mathematical, Physical and Engineering Sciences, vol. 454, p. 903, 1998.
[10] E. Delechelle, et al., "Empirical mode decomposition: an analytical approach for sifting process," Signal Processing Letters, IEEE, vol. 12, pp. 764-767, 2005.
[11] P. Flandrin, et al., "Empirical mode decomposition as a filter bank," Signal Processing Letters, IEEE, vol. 11, pp. 112-114, 2004.
[12] G. Rilling, et al., "On empirical mode decomposition and its algorithms," 2003, pp. 8–11.